Invited Paper

Large–scale Holographic Memory: Experimental Results

Geoffrey W. Burr, Fai Mok, and Demetri Psaltis

Electrical Engineering Department, MS 116–81
California Institute of Technology
Pasadena, CA 91125

ABSTRACT

We present experimental results of a page–formatted random–access holographic memory capable of storing up to 10^{12} bits of information. Up to 500 holograms were angularly multiplexed at each of 8 spatially multiplexed locations, using a mechanical scanner and a segmented mirror array.

LARGE–SCALE MEMORY

The target specifications of this large–scale memory have been presented before [1] and are only summarized here. The system design calls for a total storage capacity of 1 Terabit (10^{12}), divided into 1 million holograms of 1 million pixels each. The holograms will be spatially multiplexed among 256 locations, with 4000 holograms multiplexed at each location. The access time of any single page of information is 100 μsec, determined by the acoustic delay through the aperture of the acoustooptic deflector. Total readout rate is in excess of 1 GBit/sec (10^9 bit/sec). Recording rate, using Fe–doped $LiNbO_3$, is about 10MBit/sec with an average recording time of 0.1 seconds.

Random access to the page–formatted data is provided by the non–mechanical scanner, since the access delay is independent of the readout sequence. Finally, we point out that all the components and technologies used in constructing this memory system are currently available.

VOLUME HOLOGRAPHY

Volume holography is a well–known technology which has received a boost in recent years through improvement in crucial components such as SLMs and detector arrays and through the emergence of applications such as image processing, neural networks, and large–scale databases. Due to the 3–dimensional nature of the storage material, many pages of data may be multiplexed by changing the storage reference angle [2], wavelength [3,4], or phase code [5,6]. Recently, Mok stored 5000 angle–multiplexed holograms of 70,000 pixels each in a $2cm^3$ volume [7].

Because the gratings which constitute the stored data overlap each other, the data is densely packed yet can be conveniently accessed. However, the overlap of gratings which correspond to different output pages leads to the question of crosstalk between holograms. We have also investigated the SNR of reconstructed binary pixel holograms [1]. The SNR due to crosstalk noise and medium noise was found to be in excess of 1400. This results in a probability of error much lower than the industry standard of 10^{-12}, assuming a Gaussian error distribution. Other noise sources, such as registration error—mismatch between CCD pixels and the pixels of the reconstructed hologram, were carefully eliminated from the above measurement.

These two experiments show that a large number of holograms can be stored and recalled with low probability of error. But even with 5000 holograms in a single location, and 1 million pixels per page of information, one can store only 5 GBits of information. Since 256 MBit RAM chips will be available in

0-8194-1275-9/93/$6.00

the next few years, holographic storage will not be competitive unless it can attain Terabit capacities. In order to store 1 Terabit, it becomes necessary to spatially multiplex—to store many angle–multiplexed holograms at multiple locations.

ARCHITECTURE

Our architecture for non–mechanical spatial and angle multiplexing is shown in Figure 1. The storage medium (item 1) is a photorefractive crystal such as $LiNbO_3$. Holograms are stored at a 16 by 16 grid of locations on the crystal, with 4000 holograms per location. The functionality of this architecture was described in detail in reference [1], and is only briefly summarized.

Figure 2 shows the spatial multiplexing of the object beam in one dimension, since the other dimension is identical. Each page to be stored is first displayed at the input SLM. The size of the pages is limited by the space–bandwidth product (SBP) of the SLM. The SLM is illuminated by a plane wave whose angle of incidence is determined by the AOD. Since the light at the SLM and at the crystal are a Fourier transform pair, we can shift the location on the crystal where the information appears by changing the angle at which the SLM is illuminated. The AODs then control which location on the crystal is being written. During recording, the electrooptic phase modulators (items 7 and 8 in Figure 1) compensate the frequency shifts introduced by the AODs.

Figures 2 and 3 diagram the operation of the mirror array—Figure 2 shows selection of output location by the vertical AOD, while Figure 3 shows angle multiplexing at a spot by the horizontal AOD. The vertical AOD in the reference arm of the system (item 4 in Figure 1) steers the reference beam to the location on the crystal where a hologram is to be written. This AOD steers the collimated beam, which is then focussed onto one of the elements in the mirror array (item 6). The mirror strips are stacked in the vertical direction, but extend horizontally. Each mirror strip is tilted in both dimensions in order to redirect incident light to one of the 16×16 locations of the crystal. The deflection angle of the vertical AOD determines which mirror strip will be illuminated, which then directs the reference beam to the corresponding location on the crystal.

The horizontal AOD moves the focussed spot along the same mirror strip. This motion in the Fourier plane of the output lens results in a change of horizontal incidence angle at the crystal, without any motion of the spot itself. The horizontal AOD provides angle multiplexing at any given location, while the vertical AOD selects which location is to be illuminated.

The schematic of the mirror array is shown in Figure 4. There are 256 mirror strips—one for each location on the crystal. The mirror array is composed of 16 "tiles," each of which has 16 mirror strips cut as grooves. The change in angle between tiles and between groove faces is 0.5°. The angular change between tiles is orthogonal to the increment between grooves, allowing tilting of individual facets in both directions.

COMPONENTS

With the exception of the mirror array itself, all the components needed for the memory are commercially available. An important component not shown in Figure 1 is the laser source. Diode pumped, doubled Nd:YAG lasers are currently available at 400mW CW power, with 1W of power available within a few years.

Currently, SLMs are available with 480 by 440 pixels. But we require a spatial light modulator (SLM) with 1000×1000 pixels. With the advent of high–definition television, this product should be available in the near future. The storage medium of choice is $LiNbO_3$, since high quality crystals of this material are available and relatively inexpensive. The dark storage time is long[8], and the material can be thermally fixed so that the holograms do not decay upon readout.

The CCD output detector must also have 1 million pixels—currently, these are available with 64 output channels for a throughput rate of 1GBit/second. Laser scan lenses with SBP up to 50,000 are available, as are 16 × 16 lenslet arrays. Acoustooptic deflectors with 1000 SBP are currently available with 70-80% efficiency.

The mirror array itself has been built with blazed grating technology. This technique involves using a diamond tip to cut grooves on suitable substrates (Figure 5). The groove angles are accurately controlled by the tilt of the diamond tip with respect to the substrate. The width of each groove is set by the dimensions of the diamond itself.

EXPERIMENTAL RESULTS

The first experiment performed with the mirror array was to demonstrate simple spatial multiplexing. We used a rotating mirror to move a beam across the mirror strips and reflected the output onto a stationary grid. Some spatially multiplexed spots are shown in Figure 6. Because of the aperture of the lenses used, and because of an error made during manufacturing, only 130 of the 256 spots were accessible.

In order to create a simple setup and store holograms with the mirror array, we chose to work with the 90° geometry (Figure 7). This configuration allows maximum angular selectivity of angle–multiplexed holograms, but the long interaction length L causes a large $e^{-\alpha L}$ loss. The 90° is also convenient to work with because the reference and object beams enter separate faces.

The experimental setup we chose to use to demonstrate spatial and angular multiplexing is shown in Figure 8. No deflection is necessary in the object beam—the image is presented at the small end face of the crystal and propagates throughout its length during storage. The mirror array is used to direct reference beams to locations along the length of the crystal. Angularly multiplexed holograms are then stored at each location, and reconstructed out the far end of the crystal at the output detector. A mechanical scanner is used to move the focussed spot on the mirror array, vertically for spatial multiplexing, and horizontally for angular multiplexing.

First, 500 holograms were stored in a single 6mm diameter spot in a 0.01% Fe–doped $LiNbO_3$ crystal of dimensions 8mm × 8mm × 50mm. The average exposure time was 3.5 seconds and the average diffraction efficiency 10^{-8}. Several reconstructions are shown in Figure 9. The original transparency is shown at upper left, and was rotated 1° between each exposure.

Next, we stored 500 holograms at each of 8 spatially multiplexed spots (each 4mm in diameter) along the length of the crystal. Because of lens apertures and other effects, some reference angles did not result in recorded holograms. The average diffraction efficiency was again 10^{-8}, and the average exposure time 4.3 seconds. Several reconstructions are shown in Figure 10.

ACKNOWLEDGEMENTS

This work is funded by Rome Lab/IRAP under contract F30602–92–C–0073.

REFERENCES

1. F. Mok, D. Psaltis, and G. Burr,"Spatially– and angle–multiplexed holographic random access memory," (invited paper) SPIE—San Diego (1992), Proc. SPIE **1773c**, pg 1.

2. D.L. Staebler, J.J. Amodei, and W. Phillips, "Multiple storage of thick phase holograms in $LiNbO_3$," VII Int. Quant. Elec. Conf., Montreal, May (1972).

3. F. T. S. Yu, S. Wu, A. W. Mayers, and S. Rajan, "Wavelength multiplexed reflection matched spatial filters using $LiNbO_3$," Opt. Commun. **81,** 343 (1991).

4. G. A. Rakuljic, V. Leyva, and A. Yariv, "Optical data storage by using orthogonal wavelength–multiplexed volume holograms," Opt. Lett. **17**, 1471–1473 (1992).

5. J. E. Ford, Y. Fainman, and S. H. lee, "Array interconnection by phase–coded optical correlation," Opt. Lett. **15,** 1088 (1990).

6. C. Denz, G. Pauliat, G. Roosen, "Volume hologram multiplexing using a deterministic phase encoding method," Opt. Comm. **85**, 171–176 (1991).

7. F. H. Mok, "Angle–multiplexed storage of 5000 holograms in lithium niobate," Opt. Lett. **18**, 915–917 (1993).

8. M. P. Petrov, S. I. Stepanov, and A. V. Khomenko, **Photorefractive Crystals in Coherent Optical Systems,** *Springer Series in Optical Sciences,* Vol. 59, Springer–Verlag, 1991, pg 225.

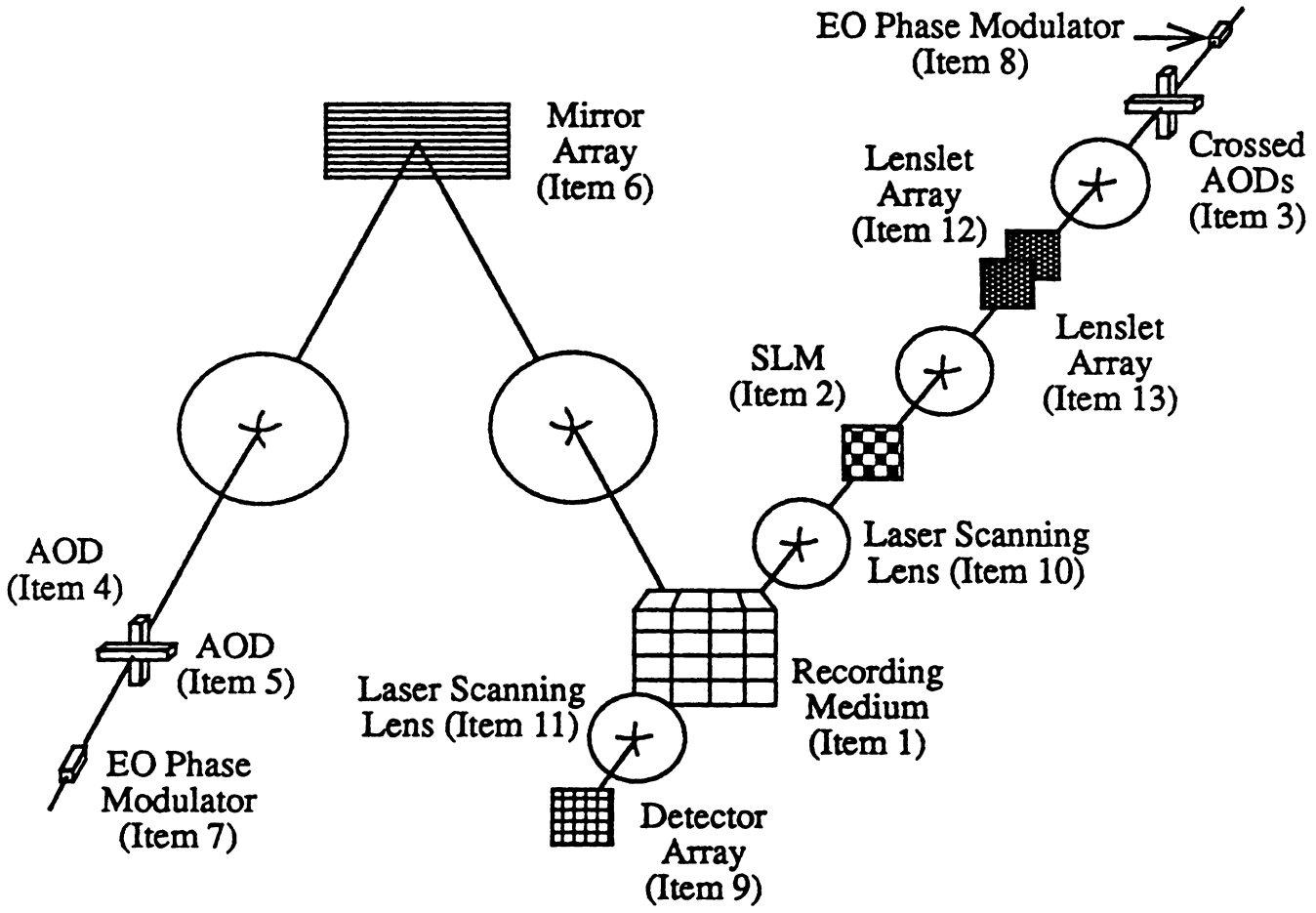

Figure 1: Schematic diagram of spatially– and angle–multiplexed holographic random access memory

SPATIAL MULTIPLEXING

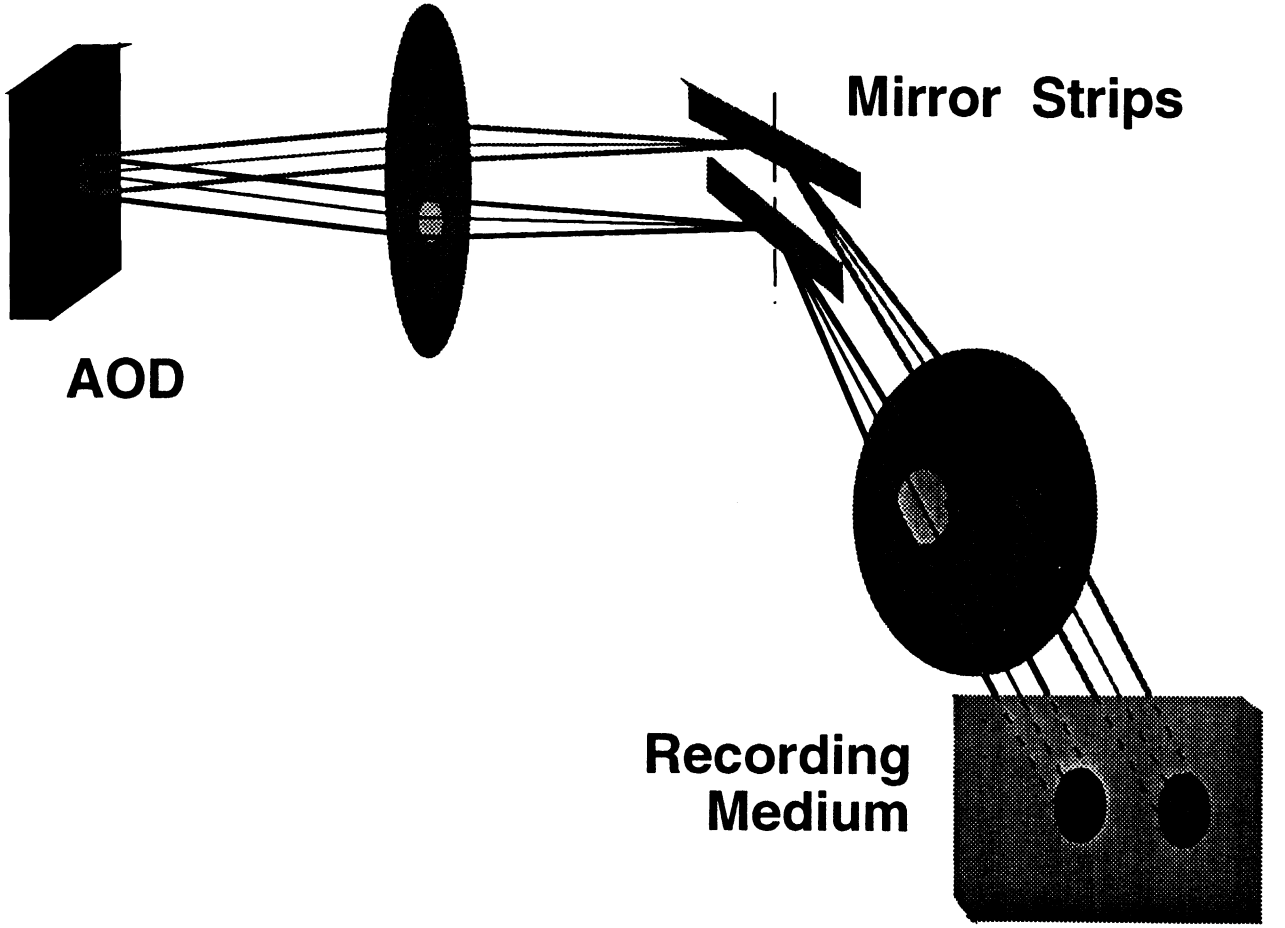

Figure 2: A two–element mirror stack, operating in conjunction with a vertically–oriented AOD and two lenses, redirects light to two distinct locations within the storage medium.

ANGLE MULTIPLEXING

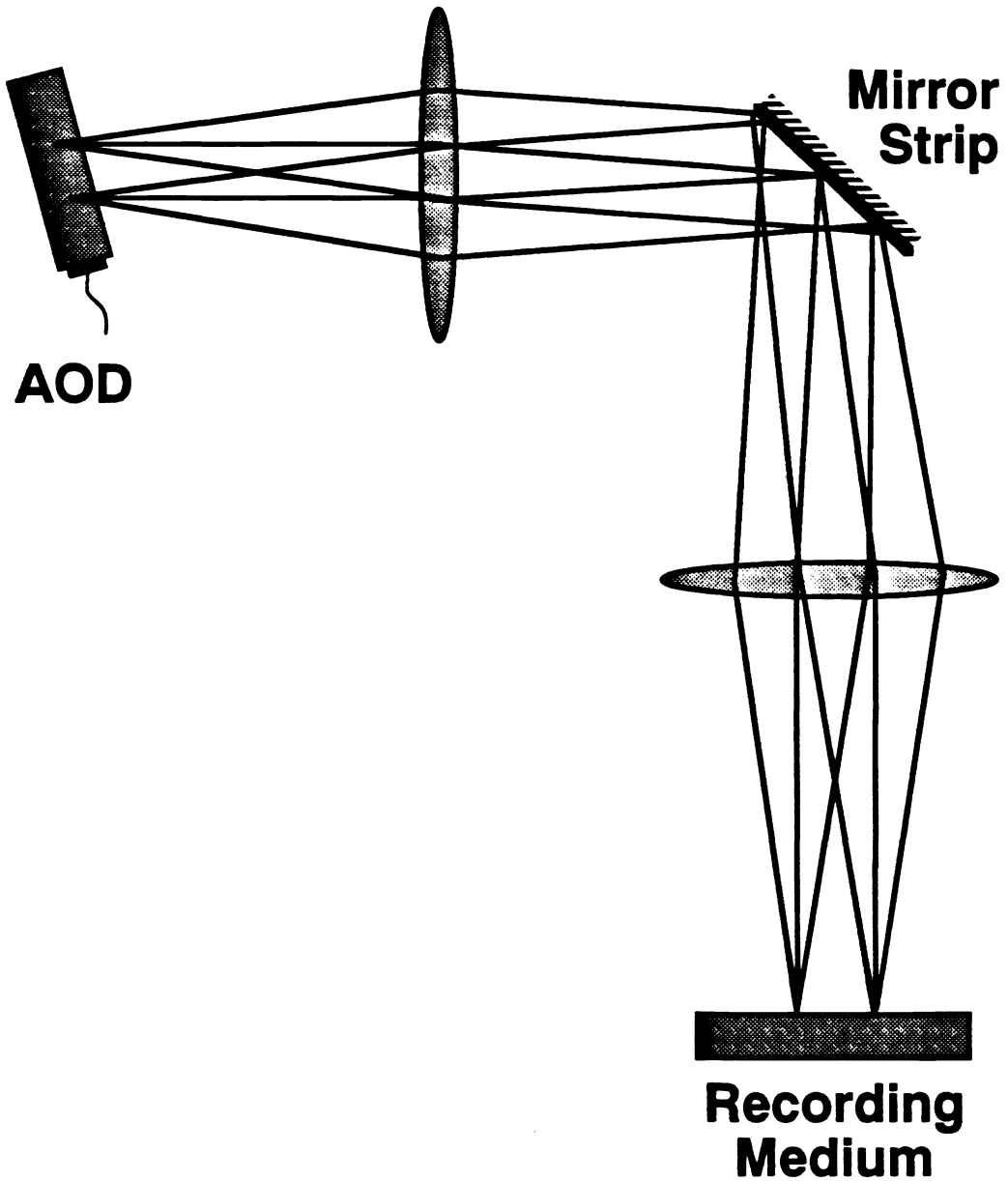

Figure 3: Schematic diagram showing three collimated beams with different angles of incidence on the storage medium. Note that all three beams stay within a common location

MIRROR ARRAY SCHEMATIC

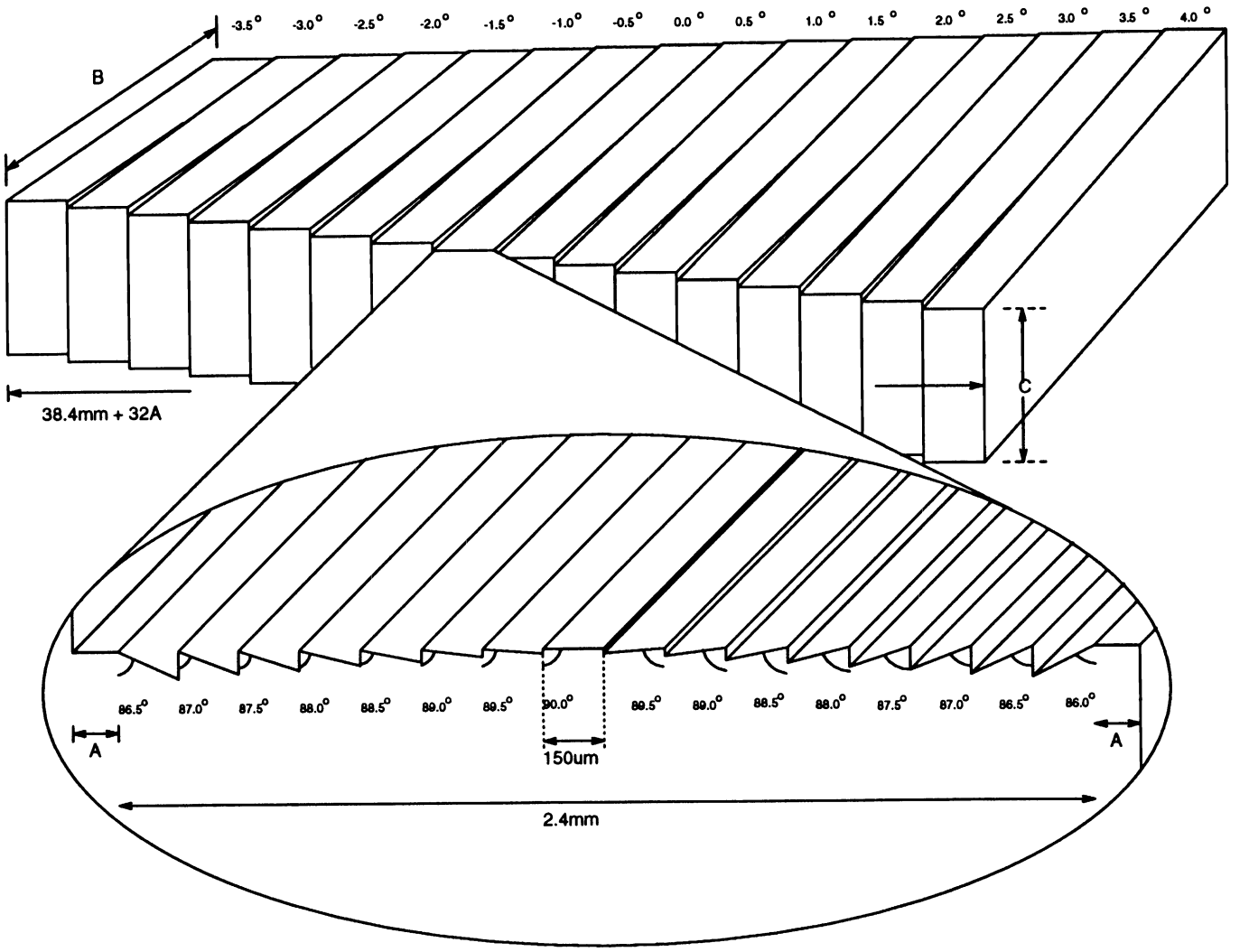

Figure 4: Schematic of mirror array. Each of the 16 tiles contains 16 facets, or grooves, each with its own tilt relative to the center facet.

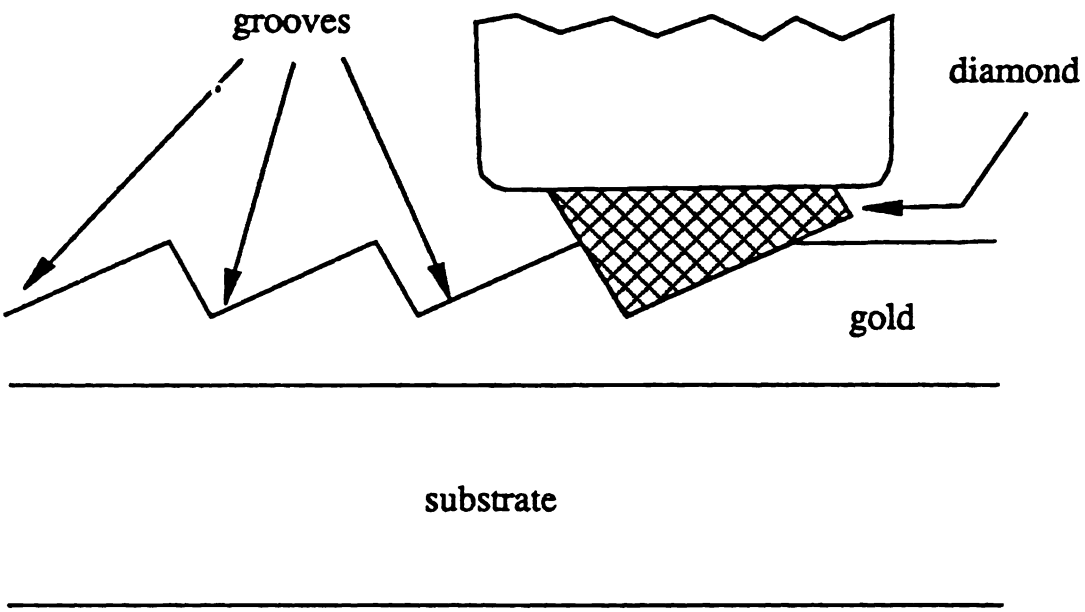

Figure 5: A simplified diagram showing the fabrication of a blazed grating

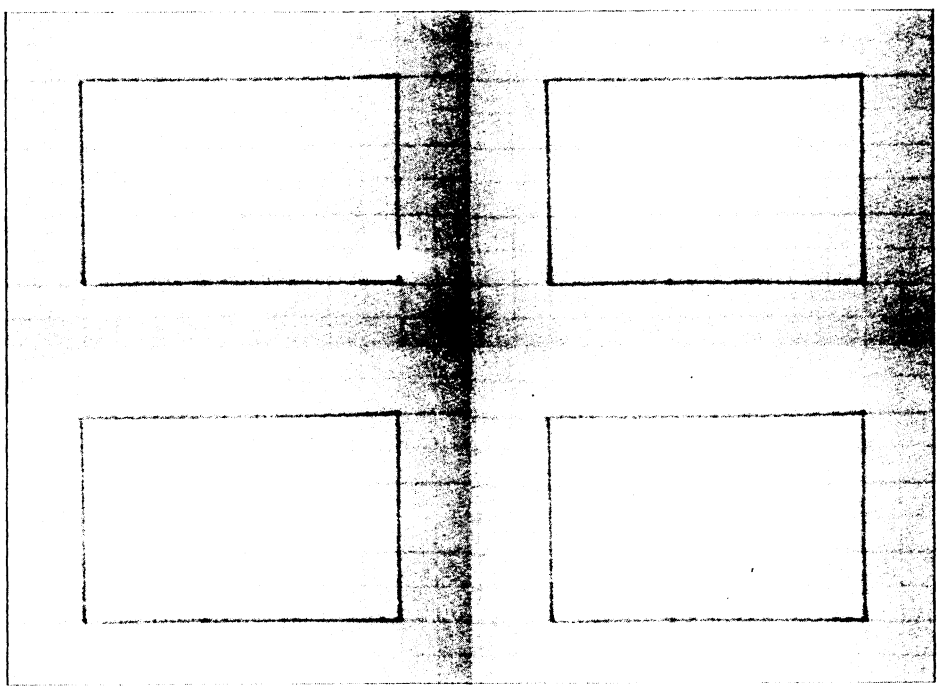

Figure 6: Examples of spatially–multiplexed reference locations

90° GEOMETRY

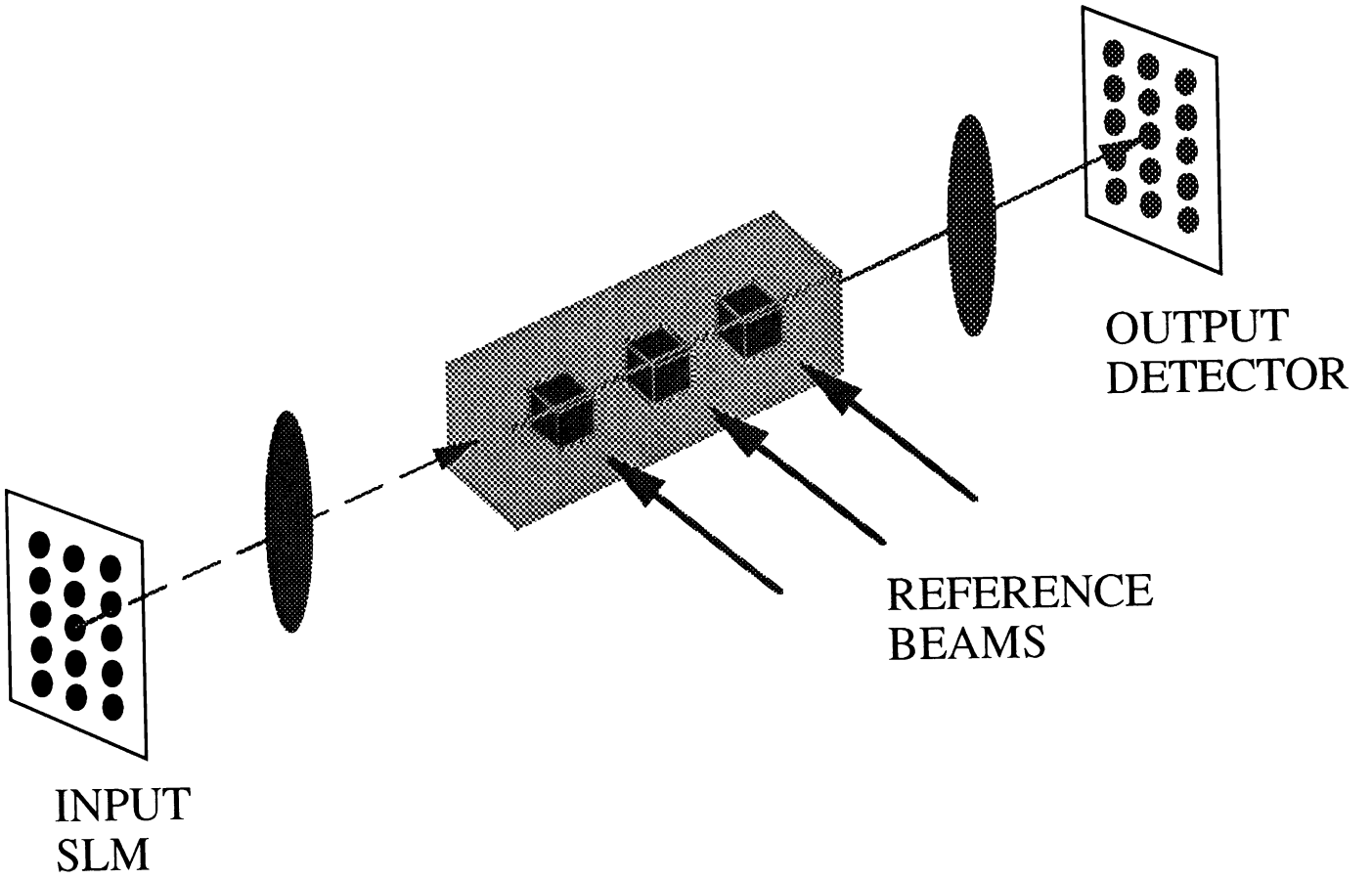

Figure 7: 90° geometry

EXPERIMENTAL SETUP

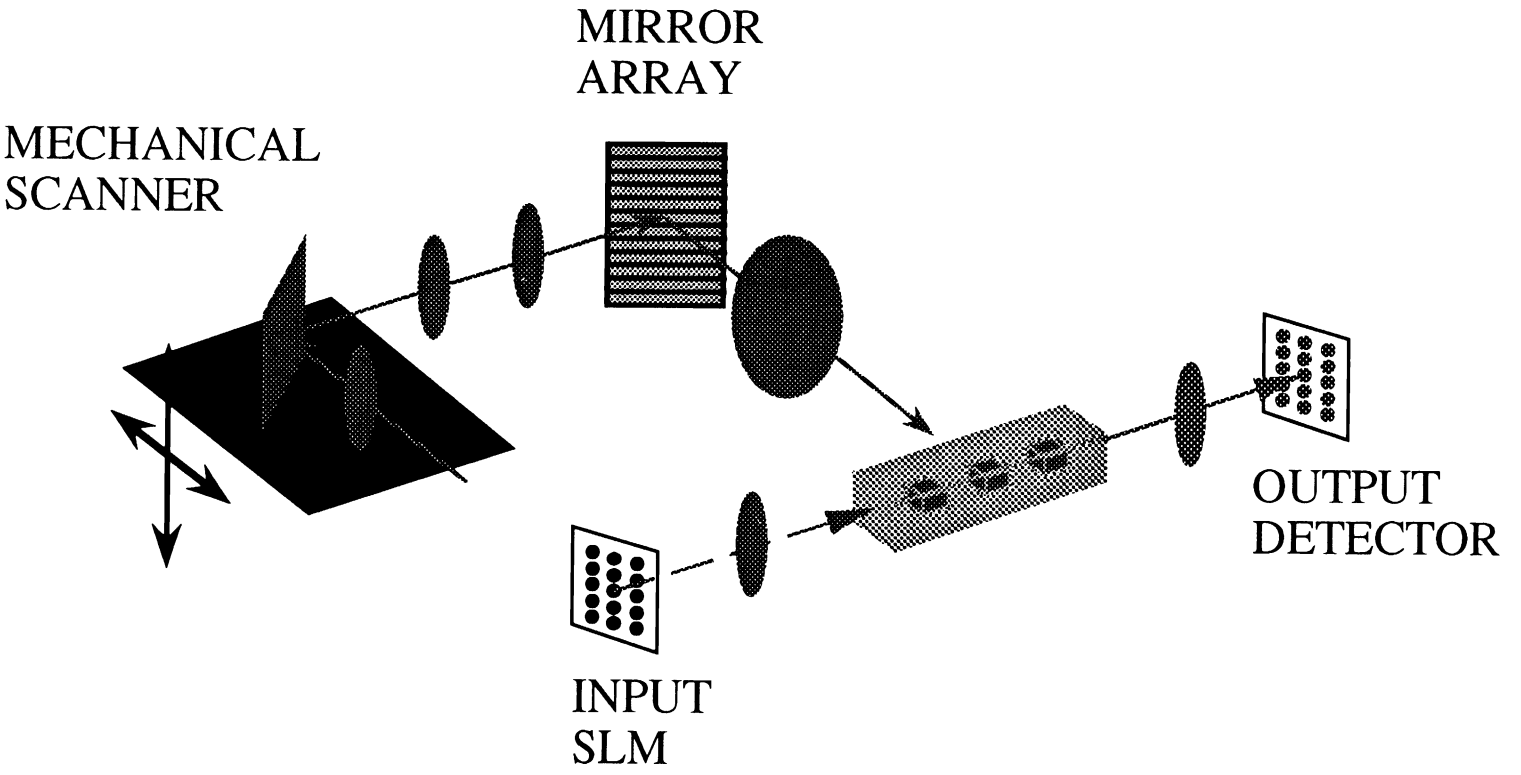

Figure 8: Experimental setup for spatial and angle–multiplexing using the 90° geometry

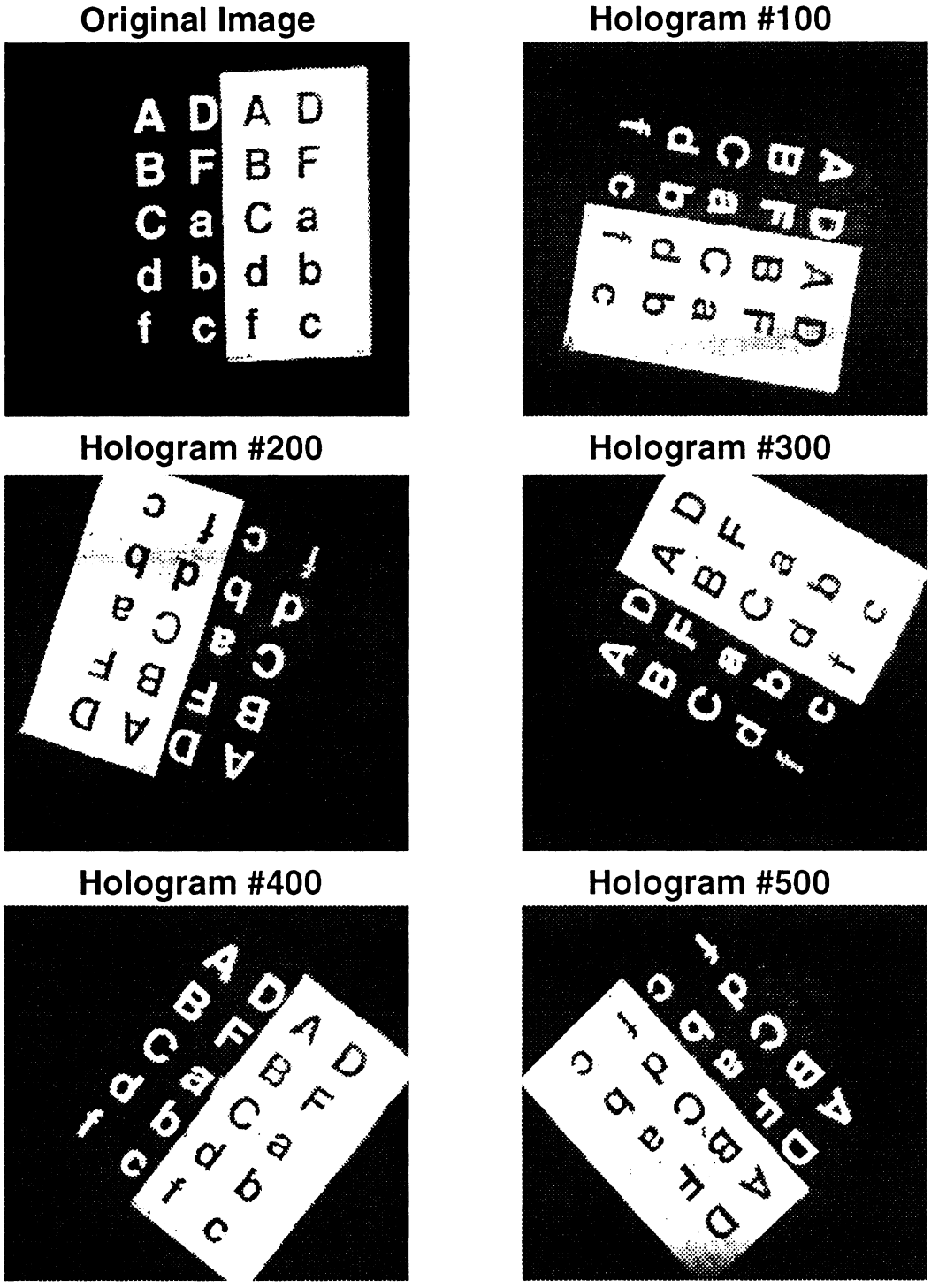

Figure 9: Example reconstructions from storage of 500 holograms at one spot

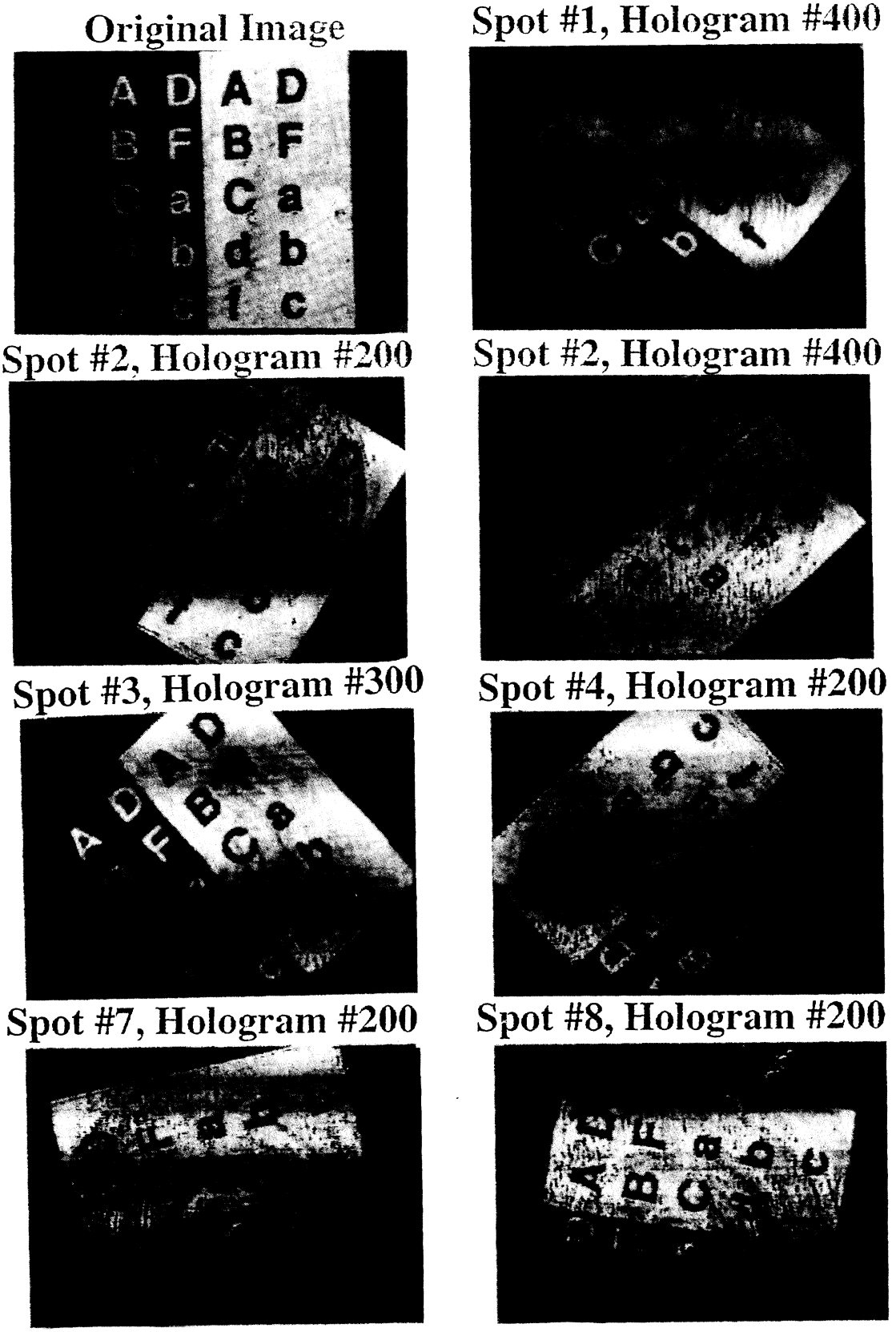

Figure 10: Example reconstructions from storage of 500 holograms at each of 8 spots